Histol Histopathol (2016) 31: 1315-1326

http://www.hh.um.es

Histology and Histopathology

From Cell Biology to Tissue Engineering

Histological assessment for femora of ovariectomized obesity (*db/db*) mice carrying mutated leptin receptor

Yusuke Tanaka[1,2], Tomoka Hasegawa[1], Tamaki Yamada[1], Tomomaya Yamamoto[1], Muneteru Sasaki[1], Hiromi Hongo[1], Kanako Tsuboi[1], Mai Haraguchi[1], Paulo Henrique Luiz de Freitas[3], Minqi Li[4], Kimimitsu Oda[5], Yasunori Totsuka[2], Kanchu Tei[2] and Norio Amizuka[1]

Departments of [1]Developmental Biology of Hard Tissue and [2]Oral and Maxillofacial Surgery, Graduate School of Dental Medicine, Hokkaido University, Sapporo, Japan, [3]Dental School, Federal University of Sergipe at Lagarto, Aracaju, Brazil, [4]Shandong Provincial Key Laboratory of Oral Biomedicine, The School of Stomatology, Shandong University, Jinan, China and [5]Division of Biochemistry, Niigata University Graduate School of Medical and Dental Sciences, Niigata, Japan

Summary. In order to provide a clue to understand the interplay between leptin and estrogen, we have examined femoral metaphyses of ovariectomized *db*/*db* mice carrying a mutated leptin receptor. We performed ovariectomy (OVX) or sham-operation (sham) on 12-week old female wild-type and *db*/*db* mice, and then, after 8 weeks, divided the animals into four groups: wild-type sham, wild-type OVX, *db*/*db* sham and *db*/*db* OVX. Samples from all groups were prepared for histochemical and ultrastructural examinations. As a result, *db*/*db* sham mice showed a reduced number and thickness of metaphyseal trabeculae and excessive adipose tissue when compared to wild-type sham mice. The wild-type OVX group exhibited markedly diminished trabecular number, as well as lower populations of osteoblasts and osteoclasts in comparison to wild-type sham group. On the other hand, trabecular numbers were similar for the two *db*/*db* groups, suggesting that the effect of the ovariectomy, i.e., estrogen deficiency may be lessened in this animal model. Leptin receptor was mainly found in osteoblasts and in bone marrow stromal cells including adipocytes. In addition, the expression of estrogen receptor did not seem to change after OVX in wild-type mice and in *db*/*db* mice. Both *db*/*db* sham and OVX mice featured many adipocytes close to the metaphyseal chondro-osseous junction, while osteoblasts accumulated glycogen granules and lipid droplets. Therefore, it seems likely that the disruption of leptin signaling in *db*/*db* mice shifts the cell differentiation cascade towards the adipocyte lineage, resulting in an osteoporotic bone independently of estrogen deficiency.

Key words: *db*/*db* mice, Overiectomy, Leptin, Osteoblast, Adipocyte

Offprint requests to: Norio Amizuka, DDS, PhD, Department of Developmental Biology of Hard Tissue, Graduate School of Dental Medicine, Hokkaido University, Kita 13 Nishi 7 Kita-ku, Sapporo, 060-8586, Japan. e-mail: amizuka@den.hokudai.ac.jp

DOI: 10.14670/HH-11-758

Introduction

Leptin was originally reported as a 16 KDa protein that is secreted by adipocytes as a product of the *ob* gene. It functions as an anti-obesity hormone that controls appetite, food intake and energy regulation (Greenberger, 1978; Zhang et al., 1994). In addition, it has been linked to lipid metabolism (Unger, 2000), cardiovascular and renal function (Hegyi et al., 2004) and bone metabolism (Ducy et al., 2000; Lee et al., 2002; Takeda et al., 2002; Williams et al., 2011). Since bone mineral density (BMD) increases along with body weight/body fat mass, some have suggested that osteoporosis and obesity may be inversely correlated (Glauber et al., 1995). The discovery of leptin and the unveiling of its functions further strengthened the idea that obesity somehow influences the regulation of bone metabolism.

In order to elucidate the effects of leptin on bone metabolism, two mice models with disruptions in leptin signaling have been reported *(ob*/*ob* and *db*/*db* mice),

both showing a similar histological phenotype in bone. Femurs of *ob*/*ob* and *db*/*db* mice had lower bone mineral content, BMD and biomechanical strength properties, including peak load, compared to wild-type mice (Ealey et al., 2006). As point mutations of the *ob* gene lead to a truncated and inactive form of leptin, the *ob*/*ob* knockout mouse is the obvious model for leptin deficiency with a phenotype comprising obesity, increased body fat mass, hyperglycemia, hyperinsulinemia, hypothermia, sterility, and impaired thyroid function (Kershaw and Flier, 2004). Another animal model, the *db*/*db* mouse, shows a point mutation in the long form of the leptin receptor, which has a long cytoplasmic domain with consensus amino acid sequences involved in binding to Janus tyrosine kinases (Greenberger, 1978; Tartaglia et al., 1995; Lee et al., 1996). Like *ob*/*ob* mice, *db*/*db* mice are obese and diabetic as consequence of leptin inactivity (Chen et al., 1996). Since *ob*/*ob* mice and *db*/*db* mice have similar bone phenotypes, they are invaluable animal models for studying leptin signaling and its relation to bone metabolism (Smith and Romsos, 1984; Takeshita et al., 1995; Steppan et al., 2000). However, the effects of leptin on bone metabolism *in vivo* seem rather unusual. There are reports of leptin acting on hypothalamic neurons to inhibit bone formation, doing so by stimulating sympathetic postganglionic neurons that reach the skeleton (central regulation by leptin) (Ducy et al., 2000; Takeda et al., 2002). On the other hand, primary cultures of human osteoblasts expressed and secreted leptin during the mineralization, thereby stimulating osteogenesis (peripheral regulation by leptin) (Thomas et al., 1999; Reseland et al., 2001). When *ob*/*ob* mice received leptin, significant increases in femoral length, total body bone area, bone mineral content and BMD could be verified (Steppan et al., 2000); thus, leptin appears to have central and peripheral effects on the skeleton.

Clarifying whether obese post-menopausal women show marked reductions in bone mass and whether there is a correlation between leptin and estrogen deficiency in the context of bone metabolism is a clinically relevant research topic. Various studies have shown differences in leptin values in pre- and post-menopausal women. In some cross-sectional studies, correlations between serum leptin and BMD in pre- and post-menopausal women could be verified (Thomas et al., 2001; Blain et al., 2002; Diegelmann, 2003). Yet, other reports indicated that post-menopausal decreases in estrogen levels do not have a direct effect on adipose tissue and leptin production (Pelleymounter et al., 1999; Kristensen et al., 2000; Martini et al., 2001; Douchi et al., 2002). Few other studies, however, compared leptin levels in women with artificially induced menopause before and after ovariectomy; when women with previously normal cycles were studied after bilateral ovariectomy, a significant reduction in leptin concentrations was found at the fourth postoperative day. Moreover, there was a positive correlation between leptin values with estradiol before and after the operation (Messinis et al., 1999). Therefore, a correlation between decreased leptin levels and estrogen deficiency might be suggested. If so, one may wonder whether leptin could rescue the reduced bone volume in post-menopausal women. One study has shown that leptin administration affected bone loss caused by estrogen deficiency by rescuing ovariectomy-induced osteoporosis in rats (Burguera et al., 2001). Taken together, all these results lead to the postulation that parallel changes in body weight, including body fat and bone mass can, at least in part, be mediated via leptin (Compston et al., 1992; Scholz et al., 1996; Yoneda et al., 2001). Leptin, therefore, seems to be in the limelight as an important player in the regulation of bone metabolism.

In this work, we have performed histochemical and ultrastructural examinations on the bone abnormalities seen in the absence of leptin signaling. Also, attempting to answer the question on whether the reduced bone volume and abnormal bone histology caused by the disrupted leptin signaling in *db*/*db* mice would be further complicated by estrogen deficiency, we performed ovariectomy (OVX) in wild-type and *db*/*db* mice, and histologically examined the post-surgical bone alterations.

Materials and methods

Animals and tissue preparation

Twelve-week old female wild-type and *db*/*db* (BKS.Cg-+Lepr^{db}/+Lepr^{db}/Jcl; CLEA Japan, Inc., Tokyo, Japan) mice (n=24 for each) were used in this study. Principles for care and research use of animals set by Hokkaido University were all strictly followed (research proposal approved under No.11-0096). First, wild-type and *db*/*db* mice (n=12 for each mice strain) were anesthetized with an intraperitoneal injection of chloral hydrate and either ovariectomized (OVX, n=6 for each mouse) or were sham-operated (sham, n=6 for each mouse). After two months, wild-type mice (wild-type sham group), ovariectomized wild-type mice (wild-type OVX group), sham-operated *db*/*db* mice (*db*/*db* sham group) and ovariectomized *db*/*db* mice (*db*/*db* OVX group) (n=6 for each group) were perfused with 4% paraformaldehyde diluted in 0.1 M cacodylate buffer (pH 7.4) through the cardiac left ventricle under anesthesia. Femora were immediately removed and immersed in the same fixative for 18 hr at 4°C. Left and right femora were decalcified with 10% ethylenediamine tetraacetic disodium salt (EDTA-2Na, for light microscopy) and 5% EDTA-2Na solution (for transmission electron microscopy, TEM), respectively. For RT-PCR analysis, femora from these four groups (n=6 for each) were extracted under anesthesia, immediately frozen with liquid nitrogen and kept at -80°C. For light microscopy, decalcified specimens were dehydrated in ascending alcohol solutions prior to paraffin embedding. For TEM observations, specimens decalcified with 5% EDTA-2Na were post-fixed with

1% osmium tetraoxide with a 0.1 M cacodylate buffer for 4 hr at 4°C, dehydrated in ascending acetone solutions, and embedded in epoxy resin (Epon 812, Taab, Berkshire, UK). Ultrathin sections were prepared with an ultramicrotome, and then stained with uranyl acetate and lead citrate for TEM observation (Hitachi H-7100 Hitachi Co. Ltd, Tokyo, Japan) at 80 kV.

Histochemistry for tissue nonspecific-alkaline phosphatase (ALP), tartrate-resistant acid phosphatase (TRAP) and multiple staining for leptin receptor/TRAP and sclerostin/ALP/TRAP

After inhibition of endogenous peroxidase activity with 0.3% hydrogen peroxidase in methanol for 30 min, dewaxed paraffin sections were pretreated with 1% bovine serum albumin (BSA; Serologicals Proteins Inc. Kankakee, IL) in PBS (1% BSA-PBS) for 30 min. Sections were then incubated for 2-3 hr at room temperature (RT) with rabbit polyclonal antisera against tissue nonspecific-alkaline phosphatase (ALP) (Oda et al., 1999) diluted at 1:300 with 1% BSA-PBS. This was followed by incubation with horseradish peroxidase (HRP)-conjugated goat anti-rabbit IgG (DakoCytomation, Glostrup, Denmark). For visualization of all immunoreactions, immune complexes were visualized using 3,3'-diaminobenzidine tetrahydrochloride (Dojindo Laboratories, Kumamoto, Japan). Enzymatic activity of tartrate-resistant acid phosphatase (TRAP) was detected as previously described (Amizuka et al., 2009); in brief, histological slides were rinsed with PBS and incubated in a mixture of 2.5 mg of naphthol AS-BI phosphate (Sigma, St. Louis, MO), 18 mg of red violet LB (Sigma) salt, and 100 mM L (+) tartaric acid (0.76 g) diluted in 30 mL of a 0.1 M sodium acetate buffer (pH 5.0) for 15 min at 37°C.

For double detection of leptin receptor and TRAP, after pre-incubation with 1% BSA-PBS for 30 min at RT, sections were incubated with rabbit polyclonal antibody against the long form of leptin receptor, OBR (Abbiotec, San Diego, CA) at 1:100 for 1hr, and then HRP-conjugated goat anti-rabbit IgG (DakoCytomation) at 1:100 for 1 hr at RT. Then, the sections were immersed in an aqueous solution of TRAP detection until the enzymatic activity was envisioned.

Regarding triple staining for sclerostin, ALP and TRAP, paraffin sections pretreated as described above were incubated with goat anti mouse sclerostin antibody (R&D systems, Inc., Minneapolis, MN) at a dilution of 1:100 in 1% BSA-PBS. The sections were subsequently reacted with ALP-conjugated anti-goat IgGs (Rockland Immunochemicals Inc., Gilbertsville, PA) at a dilution of 1: 100 at RT. Immunostained sections were immersed in an aqueous solution containing 2.5 mg of naphthol AS-BI phosphate (Sigma) and 18 mg of fast blue RR salt (Sigma) diluted in 30 mL of a 0.1 M Tris-HCl buffer (pH 8.5) for 15 min at 37°C, until immunoreactivity was envisioned. Thereafter, the slides were incubated with specific antisera to ALP, followed by incubation with HRP-conjugated secondary antibody against rabbit IgGs (DakoCytomation). Visualization of ALP immunoreactivity was performed using 3,3'-diaminobenzidine tetrahydrochloride as a substrate. After washing with PBS, theses slides were subjected to TRAP detection as described above. All sections were counterstained with methyl green, and observed under light microscopy (Eclipse E800, Nikon Instruments Inc. Tokyo, Japan).

Statistical analyses for statistic bone histomorphometrical parameters (BV/TV, Tb.N, Tb.Th, Tb. Sp, Ct.Th, N.Ob and N.Oc) and the index of adipose tissue area

Sagittal sections of the femora of the wild-type sham, wild-type OVX, *db*/*db* sham and *db*/*db* OVX groups (n=6 for each) were cut as shown in Fig. 1. The region of interest (ROI) for bone histomorphomertry is the femoral distal metaphysis neighboring the chondro-osseous junction, including the cortical bone up to an assumed horizontal line 200 μm distant from the chondro-osseous junction. Bone volume per tissue volume (BV/TV), trabecular number (Tb.N), trabecular thickness (Tb.Th), trabecular separation (Tb.Sp) and the percentage of adipose tissue area/tissue volume were evaluated for all four groups. Cortical bone thickness (Ct.Th) was expressed as an average of the cortical thickness from the chondro-osseous junction to a point 2 mm distant from the junction. As reported previously (Sasaki et al., 2013), we regarded ALP-positive cells located on bone surface as osteoblasts, while multinucleated (more than two nuclei) TRAP-reactive cells were regarded as osteoclasts. N.Ob or N.Oc was quantified using the ImagePro Plus 6.2 software (Media Cybernetics, Silver Spring, MD).

Statistical analysis

Statistical analysis was assessed by Bonferroni method, and considered statistically significant at $P<0.008$.

RT-PCR for gene expression of Alp, leptin, leptin receptor, estrogen receptor α and β, Pparγ and Pparγ2

Total RNA from femora of the wild-type sham, wild-type OVX, *db*/*db* sham and *db*/*db* OVX groups was isolated by homogenizing with 5ml TRIzol reagent (Invitrogen, Carlsbad, CA). As reported (Yoneda et al., 2001; Yamada et al., 2011; Sasaki et al., 2013), the mixture was centrifuged at 15,000 rpm for 5 min at 4°C to remove bone debris. The supernatant was transferred to a new tube, 1 ml chloroform was added, and the tube was vortexed for 15 sec. The lysate was then transferred to a new tube and incubated for 5 min at RT. After clear phase separation, the aqueous phase containing the RNA was transferred to a fresh new tube and RNA was precipitated by adding 2.5 ml isopropyl alcohol per 5ml TRIzol reagent. After 10 min incubation at RT, the mixture was centrifuged for 60 min at 15,000 rpm at

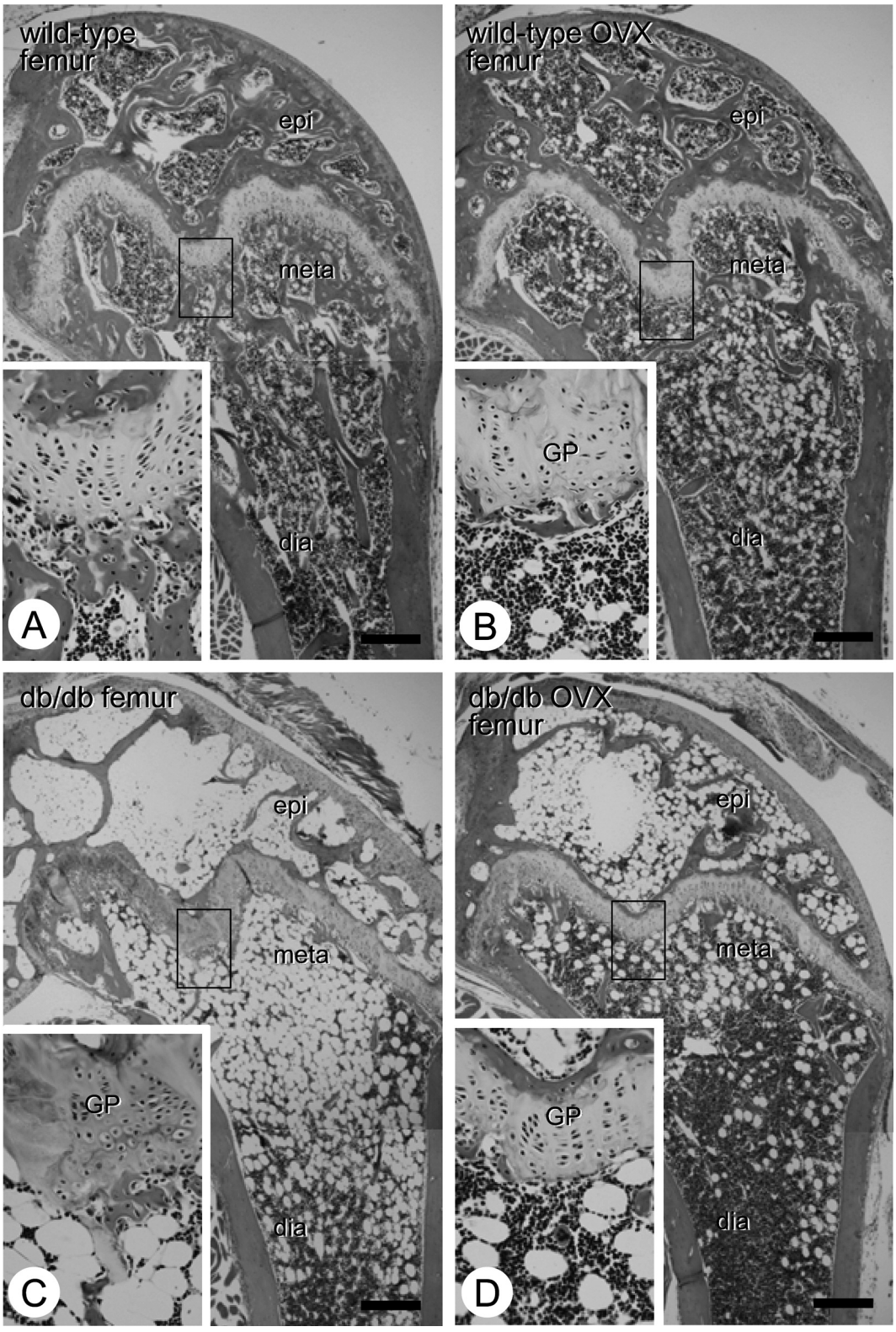

Fig. 1. Femoral histology of sham-operated or ovariectomized wild-type and *db/db* mice. Panels A and B show the sagittal sections of femora of wild-type sham-operated **(A)** and OVX **(B)**, while C and D represent those of *db/db* sham-operated **(C)** and OVX **(D)**. After OVX, wild-type femur **(B)** reveals a lower number of metaphyseal trabecules, compared to sham-operated one **(A)**. Note markedly-thinned trabecules in epiphysis and metaphysis and a huge area of adipose tissues in *db/db* femora **(C and D)**. The insets show higher magnifications of metaphysis and the growth plate, featuring less developed trabecules in wild-type OVX(B), *db/db* sham **(C)** and *db/db*OVX **(D)** femora. epi; epiphysis, meta; metaphysis, dia; diaphysis, GP; growth plate. Scale bars: 0.5 mm.

4°C. The resulting RNA pellet was washed with 1 ml 75% ethanol and was briefly air-dried. RNA was dissolved in 30 μl DEPC-treated water. First strand cDNA was synthesized from 2 μg of total RNA by SuperScript VlLO cDNA Synthesis Kit (Invitrogen).

The sequences for primers used are in Table 1. PCR was performed using a thermal cycler, as follows: denaturation at 94°C for 30 seconds, annealing at 60°C (for Gapdh), 55°C (for Alp, leptin receptor(Leptin-R), estrogen receptor(ER) α and β, Pparγ and Pparγ2) and 68°C (for leptin) for 30 seconds, extension at 72°C for 30 seconds, and a final incubation at 72°C for 10 min. RT-PCR products were subjected to 2% agarose gel electrophoresis, stained with ethidium bromide, and detected using E-Gel Imager (Invitrogen).

Results

Histological and histomorphometrical evaluation for femora of sham-operated or ovariectomized wild-type and db/db mice

In the wild-type OVX group, metaphyseal trabecular number was lower than in the wild-type sham group

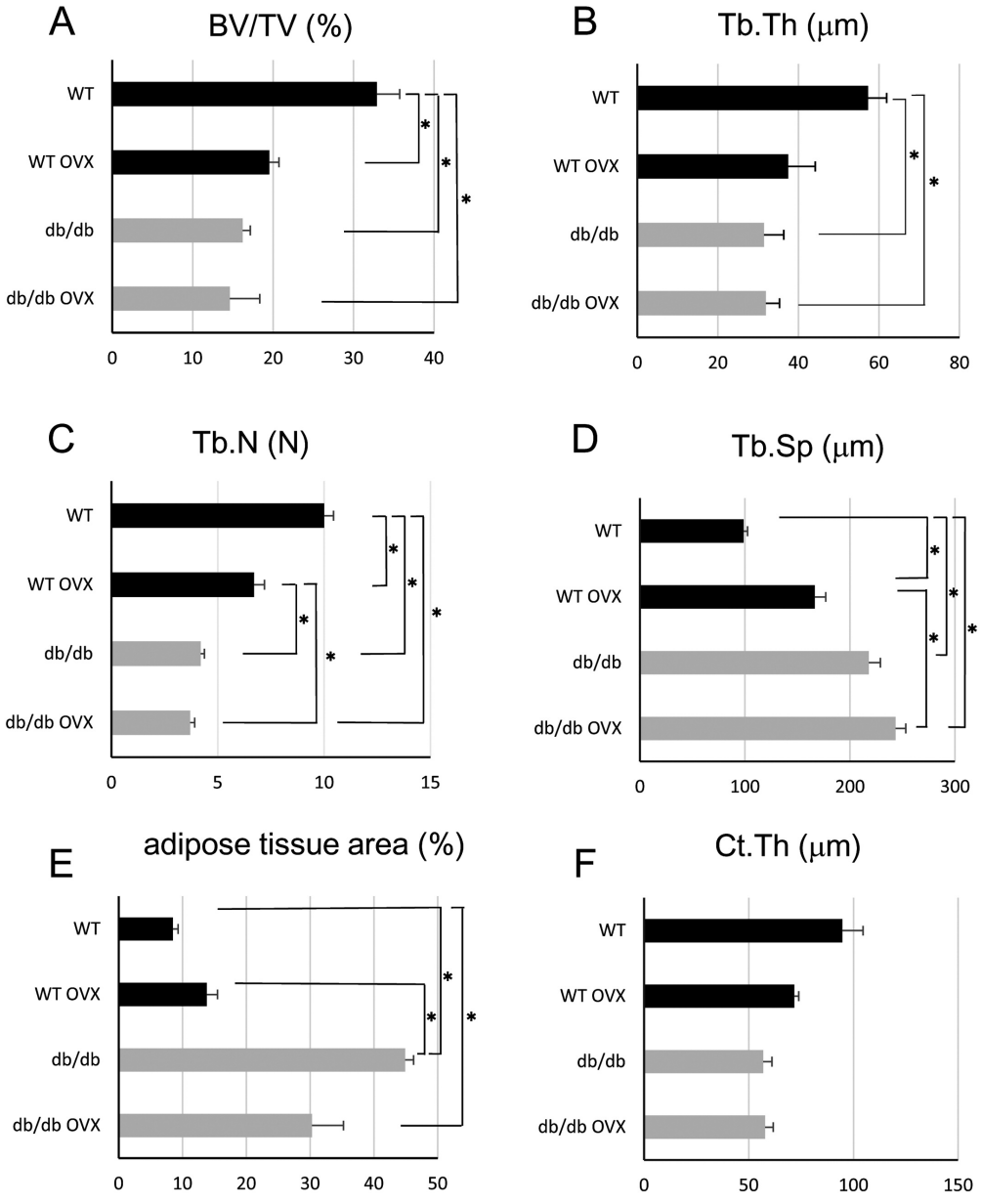

Fig. 2. Histomorphometrical evaluation on the static parameters in the femora of sham-operated or ovariectomized wild-type and *db/db* mice. Static parameters such as BV/TV (%), Tb.Th (μm), TB.N (/mm), Tb.Sp (μm), adipose tissue area/TV (%) and Ct.Th (μm) are evaluated in sham-operated and OVX groups in both wild-type (WT) and *db/db* groups (n=6 for each). The index is represented as mean±standard error. The asterisk indicates statistically significant differences assessed by Bonferroni method, and considered statistically significant at P<0.008.

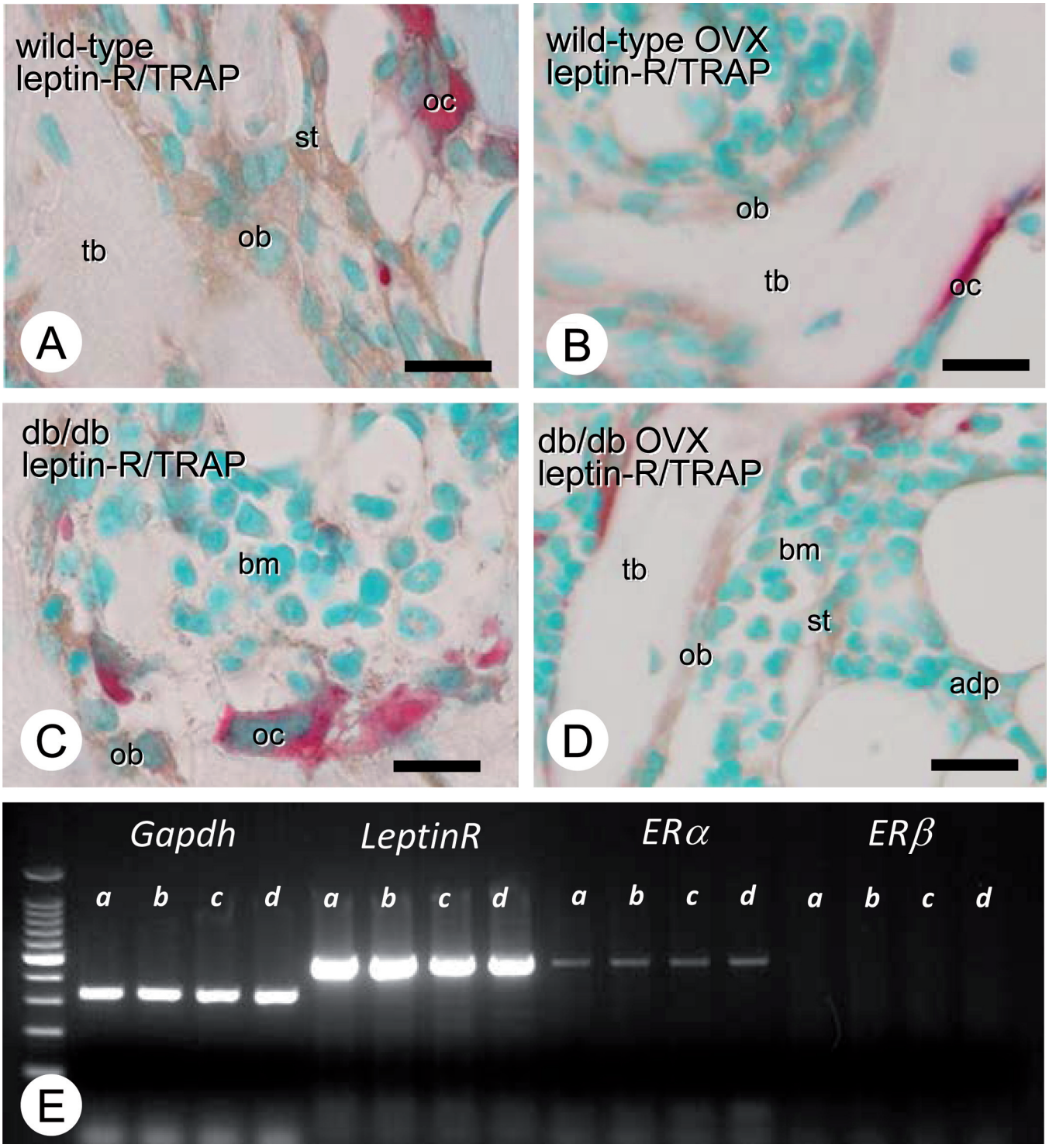

Fig. 3. Immunolocalization and gene expression of leptin receptor in the wild-type and *db/db* femora. Panels A and B show the double staining for leptin receptor (Leptin-R) and TRAP in the metaphyses of wild-type sham-operated **(A)** and OVX **(B)**, while C and D represent those of *db/db* sham-operated **(C)** and OVX **(D)**. Immunohistochemistry using antibody against the long form of leptin-R shows the leptin-R immunoreactivity (brown color) in osteoblasts (ob), bone marrow stromal cells (st) including preosteoblasts and adipocytes (adp) in both sham and OVX groups of the wild-type and *db/db* mice **(A-D)**. Osteoclasts (oc) represented as red color by TRAP detection do not possess the leptin-R immunoreactivity. RT-PCR consistently exhibits the similar expressions of Leptin-R and ERα in all the groups, while ERβ is not detectable. tb; trabecule, bm; bone marrow. Scale bars: 20 μm.

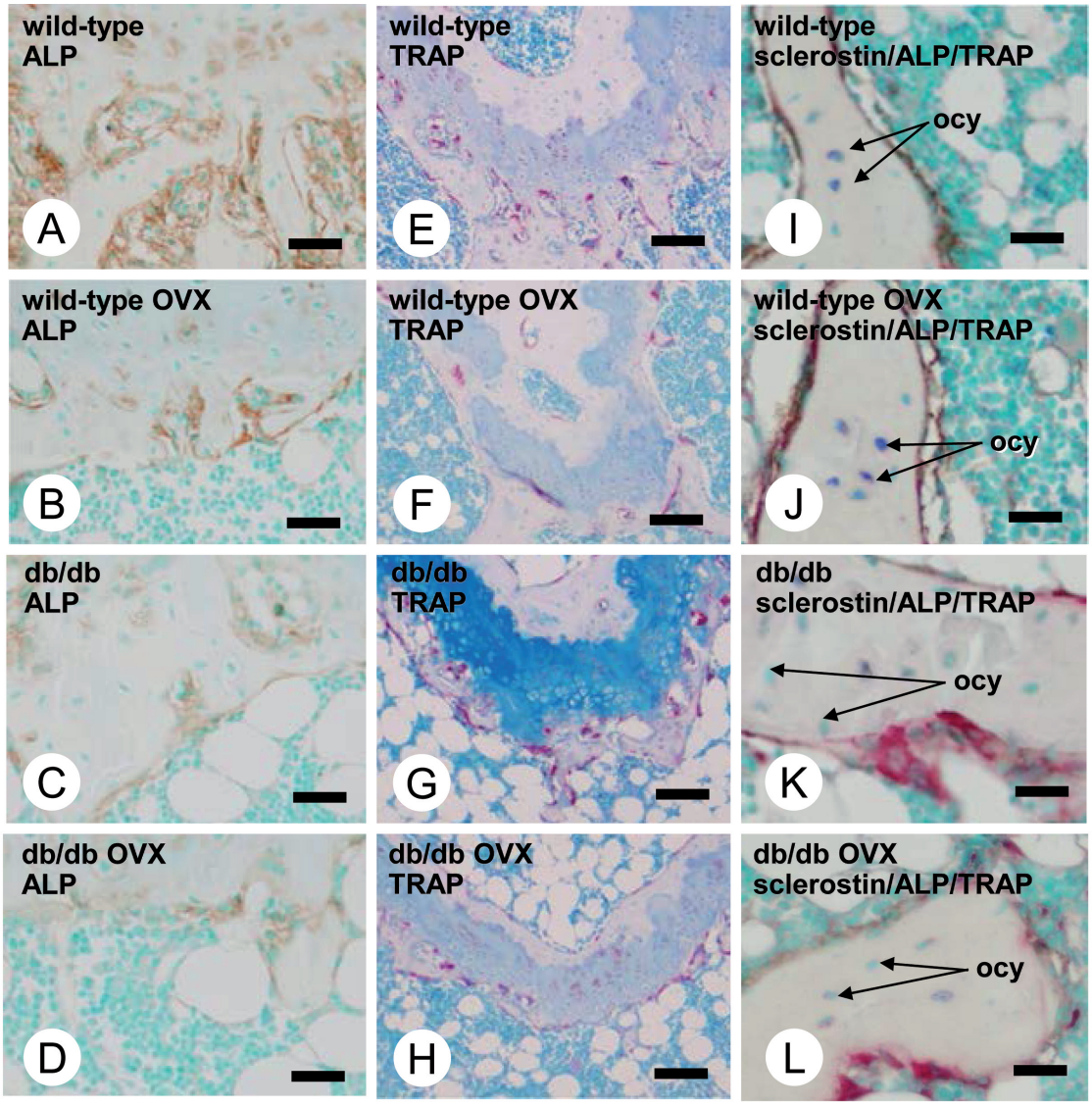

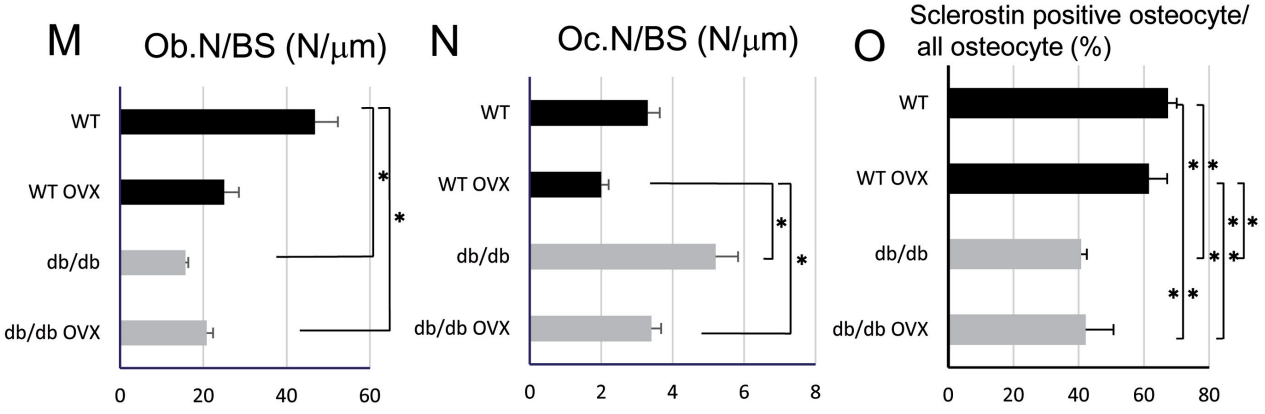

Fig. 4. Immunohistochemistry for ALP, TRAP and sclerostin in the wild-type and *db/db* femora. Panels **A-D** and **E-H** show ALP (brown color) and TRAP (red color) staining, respectively, while Panels **I-L** reveals triple staining of sclerostin (violet color), ALP (brown) and TRAP (red). Panels **A, E, I and B, F, J** are derived from wild-type sham and OVX groups, whereas panels **C, G, K and D, H, L** are *db/db* sham and OVX metaphyses. There are many ALP-positive cells in the wild-type sham metaphysis **(A)** compared to those in other groups **(B-D)**, which is consistent with statistical analysis of N.Ob/BS as shown in panel **M**. N.Oc/BS was significantly increased in *db/db* sham and OVX groups compared to wild-type OVX group, though TRAP-positive osteoclasts are seemingly lessened after OVX in wild-type **(E and F)** and *db/db* **(G and H)** metaphyses. Sclerostin immunoreactivity in osteocytes (ocy) is markedly reduced in *db/db* sham and OVX metaphyses **(K and L)** compared to those of wild-type mice **(I and J)**. Panel **O** shows the statistical analysis of the percentage of sclerostin-positive osteocyte / all osteocytes. Scale bars: A-D, 80 μm; E-H, 160 μm; I-L, 40 μm.

(Compare Fig. 1A,B). Histological findings were consistent with static parameters of bone histomorphometry, which showed a significant reduction of BV/TV (wild-type sham vs wild-type OVX; 32.93±6.92 vs 19.48±3.01, P<0.005) and Tb. N (wild-type sham vs wild-type OVX; 10.00±1.10 vs 6.67±1.21, P<0.005), as well as an extreme increase of Tb.Sp (wild-type sham vs wild-type OVX; 98.55±9.65 vs 166.47±25.35, P<0.005) (Fig. 2A,C,D). In contrast, femora of *db/db* sham mice showed marked reduction in metaphyseal trabecular number with a much higher fat content in bone marrow, compared to the wild-type femora (Compare Fig. 1A,C). These findings were confirmed by bone histomorphometry, through which significant decreases in BV/TV (wild-type sham vs *db/db* sham; 32.93±6.92 vs 16.15±4.40, P<0.005), Tb.Th (wild-type sham vs *db/db* sham; 57.32±11.37 vs 31.48±11.90, P<0.005) and Tb.N (wild-type sham vs *db/db* sham; 10.00±1.10 vs 4.17±0.41, P<0.005), and a prominent increase of Tb.Sp (wild-type sham vs *db/db* sham; 98.55±9.69 vs 217.92±26.90, P<0.005) could be verified (Fig. 2A-D). Moreover, a significant increase in adipose tissue area (wild-type sham vs *db/db* sham; 8.50±2.01 vs 44.87±3.23, P<0.005) in *db/db* mice was observed (Fig. 2E). Ct.Th also tended to be diminished in *db/db* mice compared to wild-type mice, though there was no statistically significant difference (Fig. 2F). After OVX, metaphyseal trabecular numbers were similar between *db/db* sham and *db/db* OVX mice (Fig. 1C,D). In the two *db/db* groups, differences in BV/TV, Tb.Th, Tb.N, Tb.Sp, Ct.Th and adipose tissue area did not reach significance (Fig. 2A-E). These findings point to the existence of an osteoporotic phenotype in the circumstance of leptin signaling blockade that does not seem to be further complicated by OVX.

Table 1.

mouse Gapdh	Forward 5'-TGTCTTCACCACCATGGAGAAGG-3' Reverse 5'-GTGGATGCAGGGATGATGTTCTG-3'
mouse leptin	Forward 5'- AGAGGGTCACTGGCTTGGAC -3' Reverse 5'- TCTTGGAGAAGGCCAGCAGATG -3'
mouse leptin receptor	Forward 5'- CAGATTCGATATGGCTTAAGTGG -3' Reverse 5'- GTTAAAATTCACAAGGGAAGCG -3'
mouse ERα	Forward 5'- TGCTACGTCAAGTCGGTTCC -3' Reverse 5'- TCCGGGGGTATGTAGTAGGT -3'
mouse ERβ	Forward 5'- CCAAGGGATGAGGGGAAGTG -3' Reverse 5'- CTTGTACCCTCGAAGCGTGT -3'
mouse Pparγ	Forward 5'- GCTCTACAACAGGCCTCATG -3' Reverse 5'- GCCAACAGCTTCTCCTTCTC-3'
mouse Pparγ2	Forward5'- AACTGCAGGGTGAAACTCTGGGAGATTCTC -3' Reverse 5'- GGATTCAGCAACCATTGGGTCAGCTCT -3'
mouse Alp	Forward 5'- GCCCTCTCCAAGACATATA -3' Reverse 5'- CCATGATCACGTCGATATCC -3'

Histochemistry on femora of sham-operated or ovariectomized wild-type and db/db mice

Immunoreactivity against the long form of leptin receptor was seen mainly in osteoblasts, preosteoblasts and bone marrow stromal cells including adipocytes in all four groups (Fig. 3A-D). Consistently, expression

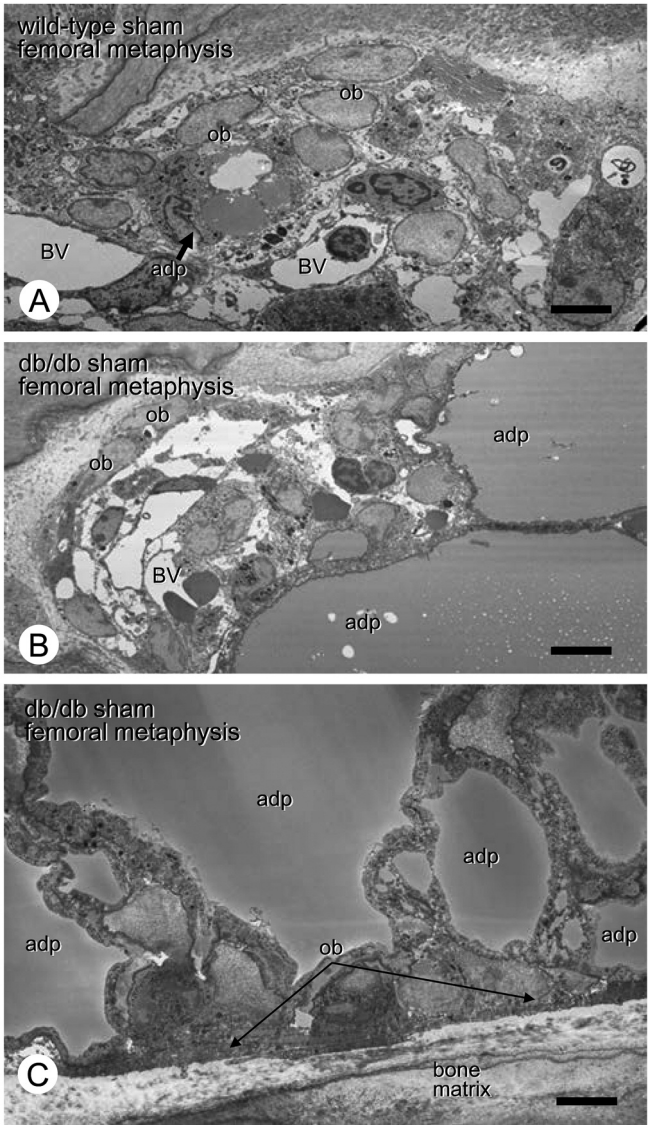

Fig. 5. Ultrastructural observation on adipocytes in the wild-type and *db/db* sham mice. Many adipocytes (adp) with huge lipid droplets are in close proximity to osteoblasts (ob) at the chondro-osseous junction of the *db/db* sham **(B)**, while the wild-type sham metaphyses show some adipocytes with small lipid droplets **(A)**. When observed at a higher magnification, *db/db* adipocytes are shown to neighbor the bone surface with intervening extremely-thinned osteoblasts (ob) in between **(C)**. BV; blood vessel. Scale bars: 10 μm.

levels for leptin receptor (*Leptin-R*) and estrogen receptor α (*ERα*) but not *ERβ* were similar in all the groups as confirmed by RT-PCR (Fig. 3E). Expression and immunolocalization of the leptin receptor, therefore, might not be affected by OVX in spite of the *db*/*db* mutation; also, the expression of *ERα* appears to be constant even with disrupted leptin signaling.

As to the immunolocalization of ALP, TRAP and sclerostin, the wild-type sham group revealed many ALP-reactive osteoblasts on the metaphyseal trabeculae, which neighbored a moderate number of TRAP-positive osteoclasts (Fig. 4A,E). However, the wild-type OVX group showed a reduction in the number of ALP-reactive osteoblasts and TRAP-reactive osteoclasts (Fig. 4B,F). On the other hand, fewer ALP-reactive osteoblasts were seen in the *db*/*db* sham group when compared to wild-type sham group (Fig. 4A,C), while the *db*/*db* sham mice still had many TRAP-reactive osteoclasts (Fig. 4G). After OVX, while the area of ALP-reactive osteoblasts did not dynamically change, TRAP-reactive osteoclasts appeared to be reduced in number in *db*/*db* mice (Fig. 4D,H). Statistical analysis showed the highest N.Ob in the wild-type sham group, but no significant differences between *db*/*db* sham and OVX groups in the same parameter (Fig. 4M). *Db*/*db* sham mice exhibited a higher index of N.Oc than did wild-type OVX mice and *db*/*db* OVX mice, the latter of which, however, had no significant difference (Fig. 4N). Staining for sclerostin - an osteocyte-derived factor inhibiting osteoblasts (Winkler et al., 2003) - was abundant in osteocytes in

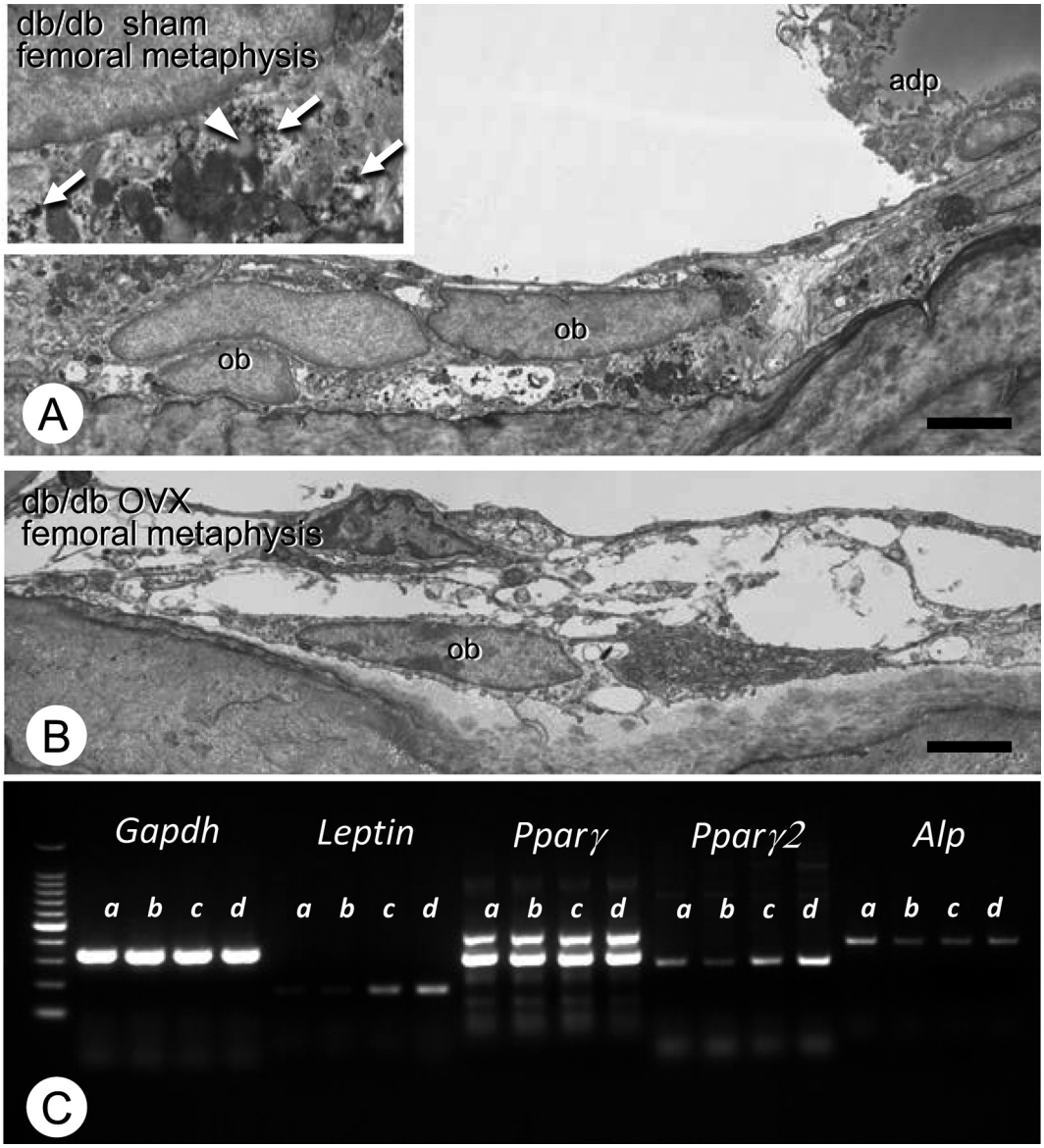

Fig. 6. Ultrastructural observation on osteoblasts and the related gene expression in *db/db* sham and OVX mice. Both *db/db* sham (**A)** and OVX **(B)** metaphyses possess flattened osteoblasts (ob) on the bone surface. When observed at a higher magnification, *db/db* osteoblasts are shown to accumulate glycogen granules (arrows) and lipid droplets (arrow head) besides developed rough endoplasmic reticulum and Golgi apparatus (See inset in A). Gene expression of Leptin, Pparγ, Pparγ2 and Alp assessed by RT-PCR are shown in panel **C.** Lines a, b, c and d indicate wild-type sham, wild-type OVX, *db/db* sham and *db/db* OVX femora. As a consequence, Leptin and Pparγ2 are intensely expressed in *db/db* sham and OVX mice, while Alp gene is only intense in the wild-type sham specimens. Adp; adipocyte. Scale bars: 5 μm.

wild-type sham and OVX groups (Fig. 4I,J). Yet, both *db*/*db* sham and OVX groups featured weak immunoreactivity for sclerostin in their osteocytes (Fig. 4K,L). Taken together, in *db*/*db* mice, osteoblastic activity seemed to be attenuated despite significantly-decreased synthesis of sclerostin (Fig. 4O).

Ultrastructural observation on osteoblasts and adipocytes in wild-type and db/db mice

Many adipocytes with huge lipid droplets were seen near the chondro-osseous junction of the *db*/*db* sham metaphyses, while the wild-type sham group showed few adipocytes that contained small lipid droplets (Fig. 5A,B). Distant from the chondro-osseous junction of the *db*/*db* specimens, many adipocytes were seen close to the bone surfaces (Fig. 5C), whereas not so many adipocytes could be seen in wild-type mice (data not shown). Alternatively, osteoblasts were shown to develop rough endoplasmic reticulum and Golgi apparatus, being involved in matrix synthesis in the wild-type sham mice. However, osteoblasts in both *db*/*db* sham and OVX mice revealed several lipid droplets associated with glycogen granules (Fig. 6A,B). Consistently, *db*/*db* sham and OVX groups showed markedly increased expression of *Leptin* and *Pparγ2* when compared to those in the wild-type sham and OVX groups (Fig. 6C). Although only the wild-type sham mice showed an intense expression of *Alp*, other groups reduced its expression (Fig. 6C).

Discussion

To our knowledge, this is the first report demonstrating the bone histology of ovariectomized *db*/*db* mice. Our study revealed that disruption of leptin signaling caused osteoporosis with an excessive amount of adipose tissue in bone marrow, a phenotype that was not made worse by estrogen deficiency.

The discovery of leptin (Greenberger, 1978) and the unveiling of its functions (Zhang et al., 1994) further strengthened the idea that obesity somehow influences the regulation of bone metabolism. Some studies showed a correlation between serum leptin and BMD in pre- and post-menopausal women (Thomas et al., 2001; Blain et al., 2002; Diegelmann, 2003), while others indicated that post-menopausal decreases in estrogen levels have no direct effect on adipose tissue or leptin synthesis (Pelleymounter et al, 1999; Kristensen et al., 2000; Martini et al., 2001; Douchi et al., 2002). Osteoporosis, however, has a wide variety of presentations, making it difficult to establish a correlation between leptin signaling and estrogen in humans. In contrast, rodent models lacking leptin signaling are useful for providing clues to the interplay between leptin and estrogen. In general, an estrogen deficiency following OVX in rodents stimulates both osteoclastic bone resorption and osteoblastic bone formation in the early stages; later, however, reductions in bone resorption and formation ultimately lead to osteoporosis. Therefore, *db*/*db* OVX mice could become osteoporotic and serve as a good model for obese post-menopausal osteoporosis.

After OVX, however, osteoporosis was not worsened in *db*/*db* mice compared to their wild-type counterparts, at least in this study, although leptin administration reduced ovariectomy-induced osteoporosis in rats (Burguera et al., 2001). This implies that histological and histomorphometrical profiles of osteoporosis induced by leptin-disruption may be more severe than those of overiectomy, revealing that the histomorphometrical parameters between *db*/*db* sham and OVX mice did not reach levels of significance as shown in Fig. 2.

We believe that disrupted leptin signaling affects bone cells differently than does estrogen deficiency. In our own study, immunoreactivity against the leptin receptor was observed in cells of the osteoblastic lineage, including preosteoblasts, bone marrow stromal cells and adipocytes (Fig. 3). In *db*/*db* mice, bone-surfacing osteoblasts revealed an accumulation of glycogen granules and lipid droplets in their cytoplasm, while *Pparγ2* and *leptin* were intensely expressed in the sham and OVX groups. In the latter group, many adipocytes accumulated near the bone surfaces (Figs. 5, 6). These findings suggest that adipocyte differentiation and function are relatively stimulated in *db*/*db* mice. In *db*/*db* bones, the blockade of leptin signaling might force undifferentiated cells towards the adipocyte differentiation ladder to the detriment of the osteoblastic one. Taking account of increased Pparγ2 gene expression, osteoblastic cells containing many lipid droplets and glycogen granules seen in the *db*/*db* sham and OVX mice might possess a part of characteristics of adipocytes (Viccica et al., 2010). The marked reductions seen in number and in thickness of metaphyseal trabeculae of *db*/*db* mice could be explained by such a differentiation shift. Thus, we postulate that leptin signaling is involved in the regulation of osteoblastic/adipocytic differentiation and function, - an idea that has been supported by the report of Thomas et al. (1999). If leptin does participate in the regulation of osteoblast/adipocyte lineages, its absence may reduce osteoblastic activities. Such an effect would prevail over that of estrogen deficiency, which affects cell coupling between osteoclasts and osteoblasts.

One may wonder why osteoblastic activity and ALP expression were reduced despite the drop in sclerostin synthesis in *db*/*db* sham and OVX mice. In fact, expression of FGF23 - another osteocyte-derived factor (Kenneth et al., 2000; Shimada et al., 2001; Kobayashi et al., 2006) - was also diminished (Tsuji et al., 2010) (data not shown). We hypothesize that osteocytic activity is also compromised by the absence of leptin signaling, and that might negatively affect osteoblastic activity. Another interesting finding was that of increased numbers of TRAP-positive osteoclasts when leptin signaling is arrested (Fig. 4). Our experiments showed that the leptin receptor is found in osteoblastic and bone

marrow stromal cells, predominantly; leptin signaling, therefore, may affect osteoclast number indirectly via osteoblastic cells. It seems fair to assume that disruptions in leptin signaling might suppress osteoblastic maturation, keeping cells at immature, preosteoblastic stages before reaching the adipocytic phenotype. These preosteoblastic cells may participate in supporting osteoclastogenesis. This is only an assumption, however, and further investigation on the role of leptin in osteoblastic/adipocytic differentiation seems necessary.

Summarizing, we performed ovariectomy in wild-type and *db/db* mice in an attempt to contribute to the understanding of the interplay between leptin and estrogen. As a consequence, leptin signaling appears to be involved in the regulation of osteoblastic/adipocytic differentiation, with the absence of leptin signaling favoring bone anabolism over the catabolic effects of estrogen deficiency.

Acknowlegements. This study was partially supported by grants from Japanese Society for the Promotion of Science (Amizuka N)

References

Amizuka N., Li M., Hara K., Kobayashi M., de Freitas P.H., Ubaidus S., Oda K. and Akiyama Y. (2009). Warfarin administration disrupts the assembly of mineralized nodules in the osteoid. J. Electron Microsc. 58, 55-65.

Blain H., Vuillemin A., Guillemin F., Durant R., Hanesse B., de Talance N., Doucet B. and Jeandel C. (2002). Serum leptin level is a predictor of bone mineral density in postmenopausal women. J. Clin. Endocrinol. Metab. 87, 1030-1035.

Burguera B., Hofbauer L.C., Thomas T., Gori F., Evans G.L., Khosla S., Riggs B.L. and Turner RT. (2001). Leptin reduces ovariectomy-induced bone loss in rats. Endocrinology 142, 3546-3553.

Chen H., Charlat O., Tartaglia LA., Woollf E.A., Weng X., Ellis SJ., Lakey N.D., Culpepper J., Moore K.J., Breitbart R.E., Duyk G.M., Tepper R.I. and Morgenstem J.P. (1996). Evidence that the diabetes gene encodes the leptin receptor: identification of a mutation in the leptin receptor gene in *db/db* mice. Cell 84, 491-495.

Compston J.E., Laskey M.A., Croucher P.I., Coxon A. and Kreitzman S. (1992). Effect of diet-induced weight loss on total body bone mass. Clin. Sci. 82, 429-432.

Diegelmann R.F. (2003). Analysis of collagen synthesis. Methods Mol. Med. 78, 349-358.

Douchi T., Iwamoto I., Yoshimitsu N., Kosha S. and Nagata Y. (2002). Leptin production in pre- and postmenopausal women. Maturitas 42, 219-223.

Ducy P., Amling M., Takeda S., Priemel M., Schilling A.F., Beil F.T., Shen J., Vinson C., Rueger J.M. and Karsenty G. (2000). Leptin inhibits bone formation through a hypothalamic relay: a central control of bone mass. Cell 100, 197-207.

Ealey K.N., Fonseca D., Archer M.C. and Ward W.E. (2006). Bone abnormalities in adolescent leptin-deficient mice. Regul. Pept. 136, 9-13.

Glauber H.S., Vollmer W.M., Nevitt M.C., Ensrud K.E. and Orwoll E.S. (1995). Body weight versus body fat distribution, adiposity, and frame size as predictors of bone density. J. Clin. Endocrinol. Metab. 80, 1118-1123.

Greenberger J.S. (1978). Sensitivity of corticosteroid-dependent insulin-resistant lipogenesis in marrow preadipocytes of obese-diabetic (*db/db*) mice. Nature 275, 752-754.

Hegyi K., Fulop K., Kovacs K., Toth S. and Falus A. (2004). Leptin-induced signal transduction pathways. Cell Biol. Int. 28, 159-169.

Kenneth E.W., Wayne EE., Jeffery L.H.O., Marcy C.S., Michael J.E., Bettina L.D., Monika G., Thomas M. and Tim M.S. (2000). Autosomal dominant hypophosphataemic rickets is associated with mutations in FGF23. Nat. Genet. 26, 345-348.

Kershaw E.E. and Flier J.S. (2004). Adipose tissue as an endocrine organ. J. Clin. Endocrinol Metab. 89, 2548-2556.

Kobayashi K., Imanishi Y., Koshiyama H., Miyauchi A., Wakasa K., Kawata T., Goto H., Ohashi H., Koyano H.M., Mochizuki R., Miki T., Inaba M. and Nishizawa Y. (2006). Expression of FGF23 is correlated with serum phosphate level in isolated fibrous dysplasia. Life Sci. 78, 2295-2301.

Kristensen K., Pedersen S.B. and Richelsen B. (2000). Interactions between sex steroid hormones and leptin in women. Studies *in vivo* and *in vitro*. Int. J. Obes. Relat. Metab. Disord. 24, 1438-1444.

Lee G.H., Proenca R., Montez J.M., Carroll K.M., Darvishzadeh J.G., Lee J.I. and Friedman J.M. (1996). Abnormal splicing of the leptin receptor in diabetic mice. Nature 379, 632-635.

Lee Y.J., Park J.H., Ju S.K., You K.H., Ko J.S. and Kim H.M. (2002). Leptin receptor isoform expression in rat osteoblasts and their functional analysis. FEBS Lett. 528, 43-47.

Martini G., Valenti R., Giovani S., Franci B., Campaqna S. and Nuti R. (2001). Influence of insulin-like growth factor-1 and leptin on bone mass in healthy postmenopausal women. Bone 28, 113-117.

Messinis I.E., Milingos S.D., Alexandris E., Kariotis I., Kollios G. and Seferiadis K. (1999). Leptin concentrations in normal women following bilateral ovariectomy. Hum. Reprod. 14, 913-918.

Oda K., Amaya Y., Fukushi-Irié M., Kinameri Y., Ohsuye K., Kubota I., Fujimura S. and Kobayashi J. (1999). A general method for rapid purification of soluble versions of glycosylphosphatidylinositol-anchored proteins expressed in insect cells: an application for human tissue-nonspecific alkaline phosphatase. J. Biochem. 126, 694-699.

Pelleymounter M.A., Baker M.B. and McCaleb M. (1999). Does estradiol mediate leptin's effects on adiposity and body weight? Am. J. Physiol. 276, 955-963.

Reseland J.E., Syversen U., Bakke I., Qviqstad G., Eide LG., Hjerther O., Gordeladze J.O. and Drevon C.A. (2001). Lepin is expressed in and secreted from primary cultures of human osteoblasts and promotes bone mineralization. J. Bone Miner. Res. 16, 1426-1433.

Sasaki M., Hasegawa T., Yamada T., Hongo H., de Freitas PH., Suzuki R., Yamamoto T., Tabata C., Toyosawa S., Yamamoto T., Oda K., Li M., Inoue N. and Amizuka N. (2013). Altered distribution of bone matrix proteins and defective bone mineralization in klotho-deficient mice. Bone 57, 206-219.

Scholz G.H., Englaro P., Thiele I., Scholz M., Klusmann T., Kellner K., Kellner K., Rascher W. and Blum W.F. (1996). Dissociation of serum leptin concentration and body fat content during long term dietary intervention in obese individuals. Horm. Metab. Res. 28, 718-723.

Shimada T., Mizutani S., Muto T., Yoneya T., Hino R., Takeda S., Takeuchi Y., Fujita T., Fukumoto S. and Yamashita T. (2001). Cloning and characterization of FGF23 as a causative factor of

tumor-induced osteomalacia. Proc. Natl. Acad. Sci. USA 98, 6500-6505.

Smith C.K. and Romsos D.R. (1984). Cold acclimation of obese (*ob/ob*) mice: effects on skeletal muscle and bone. Metabolism 33, 858-863.

Steppan C.M., Crawford D.T., Chidsey-Frink KL., Ke H. and Swick AG. (2000). Leptin is a potent stimulator of bone growth in *ob/ob* mice. Regul. Pept. 92, 73-78.

Takeda S., Elefteriou F., Levasseur R., Liu X., Zhao L., Parker K.L., Armstrong D., Ducy P. and Karsenty G. (2002). Leptin regulates bone formation via the sympathetic nervous system. Cell 111, 305-317.

Takeshita N., Mutoh S. and Yamaguchi I. (1995). Osteopenia in genetically diabetic *DB/DB* mice and effects of 1alpha-hydroxyvitamin D3 on the osteopenia. Basic Research Group. Life Sci. 56, 1095-1101.

Tartaglia L.A., Dembski M., Weng X., Deng N., Culpepper J., Devos R., Richards G.J., Campfield L.A., Clark FT., Deeds J., Muir C., Sanker S., Moriarty A., Moore K.J., Smutko J.S., Mays G.G., Wool E.A., Monroe C.A. and Tepper R.I. (1995). Identification and expression cloning of a leptin receptor, OB-R. Cell 83, 1263-1271..

Thomas T., Gori F., Khosla S., Jensen M.D., Burguera B. and Riggs B.L. (1999). Leptin acts on human marrow stromal cells to enhance differentiation to osteoblasts and to inhibit differentiation to adipocytes. Endocrinology 140, 1630-1638.

Thomas T., Burguera B., Melton L.J. 3rd, Atkinson E.J., O'Fallon W.M., Riggs B.L. and Khosla S. (2001). Role of serum leptin, insulin, and estrogen levels as potential mediators of the relationship between fat mass and bone mineral density in men versus women. Bone 29, 114-120.

Tsuji K., Maeda T., Kawane T., Matsunuma A. and Horiuchi N. (2010). Leptin stimulates fibroblast growth factor 23 expression in bone and suppresses renal 1alpha,25-dihydroxyvitamin D3 synthesis in leptin-deficient mice. J. Bone Miner. Res. 25, 1711-1723.

Unger R.H. (2000) Leptin physiology: a second look. Regul. Pept. 92, 87-95.

Viccica G., Francucci C.M. and Marcocci C. (2010) The role of PPARγ for the osteoblastic differentiation. J. Endocrinol. Invest. (7 Suppl), 9-12.

Williams G.A., Callon K.E., Watson M., Costa J.L., Ding Y., Dickinson M., Wang Y., Naot D., Reid I.R. and Comish J. (2011). Skeletal phenotype of the leptin receptor-deficient *db/db* mouse. J. Bone Miner. Res. 26, 1698-1709.

Winkler D.G., Sutherland M.K., Geoghegan J.C., Yu C., Hayes T., Skonier J.E., Shpektor D., Jonas M., Kovacevich B.R., Staehling-Hampton K., Appleby M., Brunkow M.E. and Latham J.A. (2003). Osteocyte control of bone formation via sclerostin, a novel BMP antagonist. EMBO J. 22, 6267-6276.

Yamada T., Tsuda M., Takahashi T., Totsuka Y., Shindoh M. and Ohba Y. (2011). RANKL expression specifically observed *in vivo* promotes epithelial mesenchymal transition and tumor progression. Am. J. Pathol. 178, 2845-2856.

Yoneda T., Maruyama Y., Uji Y., Motomiya Y., Hashiquchi Y., Miura M., Kitajima I. and Maruyama I. (2001). A possible role for leptin in normo- or hypoparathyroid uremic bone in postmenopausal dialysis women. J. Bone Miner. Metab. 19, 119-124.

Zhang Y., Proenca R., Maffei M., Barone M., Leopold L. and Friedman J.M. (1994). Positional cloning of the mouse obese gene and its human homologue. Nature 372, 425-432.

Accepted March 17, 2016